Talanta 121 (2014) 43–49

Contents lists available at ScienceDirect

Talanta

journal homepage: www.elsevier.com/locate/talanta

A cataluminescence-based vapor-sensitive sensor array for discriminating flammable liquid vapors

Bowei Liu [a], Hao Kong [b], Aiqin Luo [a,*]

[a] School of Life Science, Beijing Institute of Technology, Beijing 100081, PR China
[b] Beijing Key Laboratory for Microanalytical Methods and Instrumentation, Department of Chemistry, Tsinghua University, Beijing 100084, PR China

ARTICLE INFO

Article history:
Received 2 August 2013
Received in revised form
24 December 2013
Accepted 26 December 2013
Available online 2 January 2014

Keywords:
Cataluminescence (CTL)
Sensor array
Nanoparticle
Flammable liquid (FL)
Vapor
Pattern recognition

ABSTRACT

This paper describes a cataluminescence-based (CTL-based) vapor-sensitive sensor array containing 10 kinds of catalytic nanoparticles for rapid detection and discrimination of 10 flammable liquid (FL) vapors. The catalytic nanoparticles are directly deposited on heating filaments with the formation of the sensing elements. When the vapor samples are imported to the sensor array with carrier gas, the CTL intensity varies with the nanoparticles. The fingerprints of 10 FL vapors are discriminated according to the distinct CTL response patterns through a linear discriminant analysis (LDA) and hierarchical cluster analysis (HCA) in SPSS (version 16.0). The canonical patterns are clearly clustered into 10 different groups with a classification accuracy of 100%. The sensor array also applies to several real-world samples. Two kinds of simulated actual vapors, originating from the combustion of carpet in the presence and absence of gasoline, can be effectively distinguished. The developed CTL-based vapor-sensitive sensor array offers a new strategy for the rapid detection of FL vapors owing to its stability, reversibility, portability and low costs.

1. Introduction

Flammable liquids (FLs) are liquids that can catch fire and are present in almost every workplace. Analysis of FLs has been performed and developed due to a great demand in environmental monitoring, food industry, biomedical engineering and especially in public security [1–4]. The most common analytical methods, such as gas chromatography/mass spectroscopy (GC/MS) and gas chromatography/flame ionization detection (GC/FID) [4], to discriminate flammable liquids are spectroscopic techniques, often coupled with chromatographic methods. Although these methods ensure high sensitivity, they usually involve sample pretreatment and are time-consuming.

An additional methodology to detect FLs is using accelerant detection canines. In a fire scene, the presence of the FL residues is one of the most important criteria to determine arsons, and therefore detection of FLs is crucial to fire investigations. The fire investigators usually use canines as gas sensors to detect trace evidences in complex circumstances [5]. However, the use of canines in detection is limited because of their vulnerability to chemical damage and high training cost.

Artificial olfactory systems, known as “artificial noses”, can be implemented to detect odors based on a sensing strategy similar to the mammalian olfactory system [6–8]. These kinds of artificial noses employ an array of broadly cross-reactive sensors which consist of a series of nonselective receptors for a wide range of chemical compounds response and diverse mixtures of possible analyte discrimination [9]. To date, numerous artificial noses such as surface acoustic wave resonators [10,11], quartz crystal resonators [12], densely integrated chemiresistor [13], optical-fiber arrays [14,15], surface plasmon resonance-based sensors [16,17], colorimetric sensors [18,19] and so on, have been developed to exploit a wide range of sensing schemes. Despite several successful applications, these artificial noses have some limitations, such as high cost, short lifetime, low stability and irreversible responses. Hence, it is necessary to develop a new strategy for vapor sensing.

Cataluminescence (CTL) is a kind of chemiluminescence emission during catalysts oxidation of flammable gases on the surface of solid catalysts in an atmosphere. CTL was first observed by Breysse et al. through a catalytic oxidation of carbon monoxide on thoria surface [20]. Our group applied a series of catalytic nanoparticles for CTL detection of organic compounds [21–27] due to nanoparticles′ high surface area, good adsorption characteristics, and high catalytic activity. The mechanism of CTL emission is caused by recombinant radiation and radiation from excited species. The analytes on the surface of nanoparticles are oxidized catalytically by oxygen in the air. The released energy of the catalytic reaction is absorbed by some of the reaction products, forming excited intermediates which decay with light emission from excited state to the ground state. Many nanoparticles have

* Corresponding author.
E-mail address: bitluo@bit.edu.cn (A. Luo).

0039-9140/$ - see front matter © 2014 Elsevier B.V. All rights reserved.
http://dx.doi.org/10.1016/j.talanta.2013.12.059

been used for CTL catalysts [28–32]. In previous studies, both individual and cross-reactive sensors have been applied for detection of volatile organic compounds and explosive gases [24,25,33–35]. Recently, a CTL sensor array based on three nanoparticles was proposed for the first time for the quantitative analysis of xylene isomers [36]. Cao's group developed a novel CTL sensing method based on simultaneous detection of the luminescent intensities of both the analyte and its products. They also used their method to identify volatile organic compounds at different concentrations [37]. CTL-based sensors hold the promise of achieving both satisfactory sensitivity and good reversibility [21,35]. They are also fast detection approaches with simple and low-cost devices. However, thus far, there is no report of a CTL-based sensor array for the detection and discrimination of FL vapors. Recently, Walt et al. achieved high classification accuracy of vapor samples throughout the field tests using a fluorescence-based cross-reactive sensor [38–40], which encourages us to study whether the sensing array strategy of CTL can be used in "artificial noses" for discrimination of FL vapors.

This paper presents an exploratory study into FL vapors detection by a CTL-based artificial nose system. The distinct CTL responses of 10 kinds of FL samples, including gasoline, which is considered as a common arson accelerant [4], were tested by sensor array and the outcomes were well discriminated by using liner discriminant analysis (LDA) and hierarchical cluster analysis (HCA). We also successfully discriminated the combustion residues of carpet with gasoline and without gasoline. This rapid and efficient strategy might be performed as a safety method to detect hazardous liquids.

2. Experimental section

2.1. Sensor formation and nanoparticles

A schematic diagram of the CTL-based array is shown in Fig. 1, illustrating the main features of the experimental apparatus for the study. The array system was fabricated by 10 home-made heating filaments (i.d.=0.5 mm, length=10 mm), the temperature of which was controlled by a transformer adjusting heating voltage (0–250 V, 50 Hz). A portion weighing 2 mg of each kind of nanoparticles was dissolved separately in 1 mL deionized water. The resolution was mixed homogeneously by vortex mixer (QL-901, Kylin-Bell Lab Instruments Co., Ltd.) for 30 s. Then 10 home-made heating filaments were fixed to the circular PTEF platform (diameter=90 mm) after being soaked in the solution for 3 min to form a layer with a thickness of about 0.1 mm (Fig. S1). The sensing elements were uniformly distributed and the CTL signals from each sensing elements were sequentially recorded by the PMT (CR-105 photomultiplier tube made by Hamatasu). Therefore, the order of sensing elements would not affect the detected results. The filter of PMT is selected to reduce thermal radiation. According to the previous research [35], different nanoparticles have different optimal wavelengths. Since the array system contained 10 kinds of nanoparticles as sensor elements, it is not feasible to install just one type of filter. As an alternative, the heating filament was chosen due to its capability of measuring the highest signal at longer wavelengths without optical filters. As a result, the PMT in our array system was without optical filters and without wavelengths discrimination.

Four nanoparticles MgO, ZrO_2, CaO and γ-Al_2O_3 ($d\sim20$ nm) were supplied by Nanjing Haitiai. Nano. Co., Ltd. $Ce(NO_3)_{36}H_2O$ (ZSM-8) and $Ni(NO_3)_{26}H_2O$ (ZSM-4) were obtained from Gymnastics Zibo Chemical Technology Development Co. Ltd. Al_2O_3–$Ba(NO_3)_2$–εu, Ag–BaO–Al_2O_3 and $Ba_3(PO_4)_2$ were synthesized by our initial study according to the reports [23,41]. A simple method was used to synthesize the Pt–BaO–Al_2O_3 nanoparticles. Specifically, Pt–Al_2O_3 was synthesized by dipping γ-Al_2O_3 ($d\sim20$ nm) in chloroplatinic acid solution for 12 h, followed by stirring for 1 h at 80 °C, exsiccation for 12 h, and calcination for 5 h at 500 °C. Pt–Al_2O_3 was dissolved in barium acetate solution for 12 h and stirred for 1 h at 80 °C, then exsiccated for 12 h and calcination for 5 h at 500 °C. The SEM images of three kinds of nanoparticles are supplied in Fig. S2. After heating the filaments with nanoparticles, the surface morphology of nanoparticles was not changed because the heating temperature was lower than the synthesis temperature.

2.2. Vapor delivery system

Vapor samples were injected into a 100 mL bottle and separately presented to sensor array with carrier gas by the delivery system. The proportion of the carrier gas and the vapor samples would affect the responses of CTL. By fixing a flow rate of the

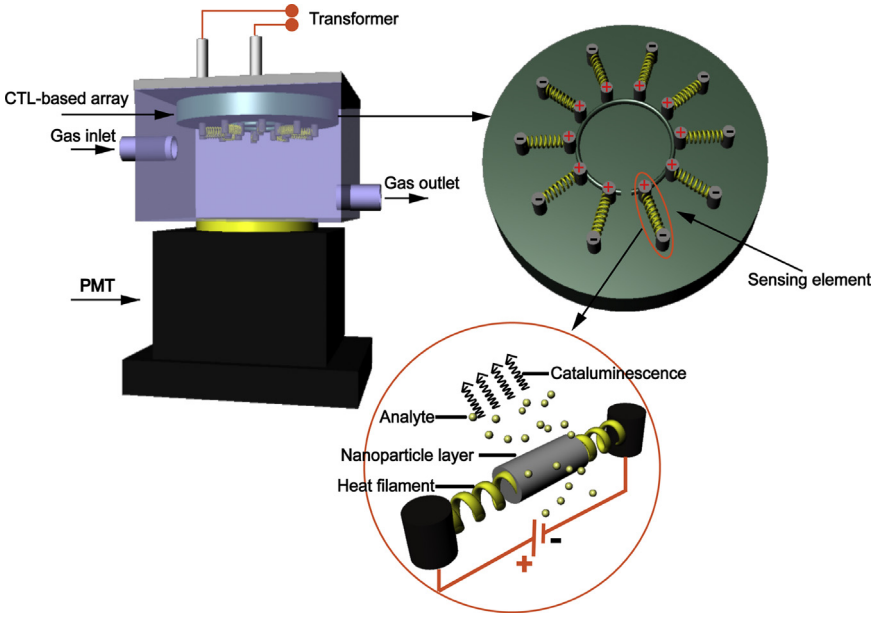

Fig. 1. Schematic diagram of the CTL-based sensor array.

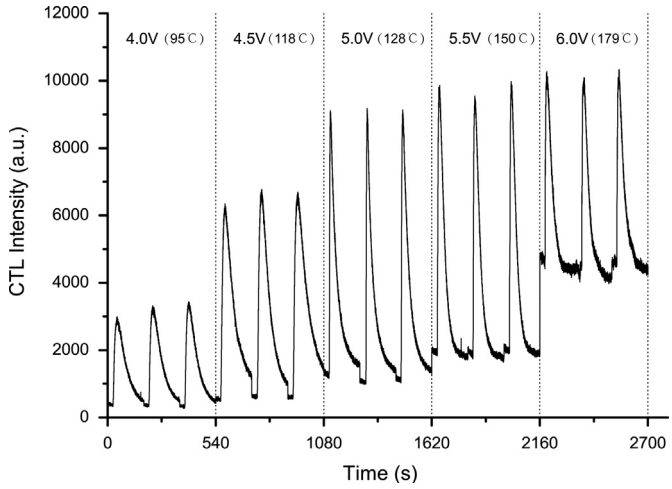

Fig. 2. The CTL intensities of 2000 ppm ethanol vapors on ZrO_2 at a heating voltage of 4.0–6.0 V. The temperature was measured by a thermocouple (SRNM-0, Shanghai Feilong Meters & Electronics Co., Ltd). Gas flow rate: 140 mL min^{-1}.

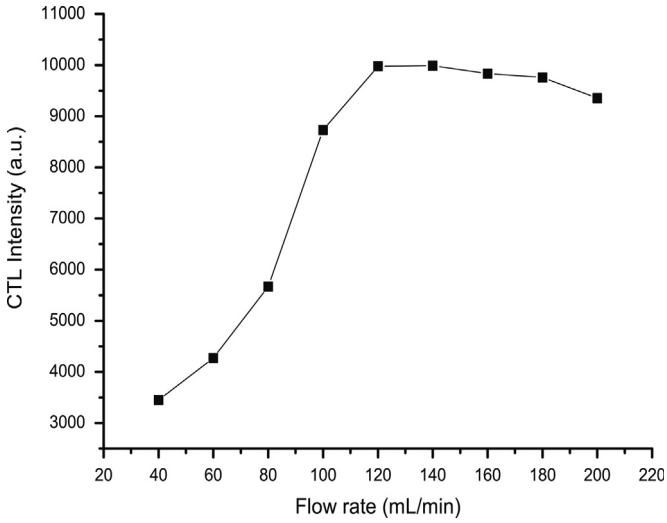

Fig. 3. Effect of flow rate of carrier gas on CTL intensity of ethanol vapor.

carrier gas, we managed to maintain a concentration of 2000 ppm for the vapor samples. An air pump (KJ-B, Tianjin Limaihao Industrial Trade Co. Ltd.) provided a steady air flow stream as carrier gas at the flow rate from 40 to 200 mL min^{-1}. The air gas was dehydrated through the silica gel column before flowing out of the pump. A flowmeter (Beijing Keyi Laboratory Instrument Co. Ltd., Beijing, China) was used to measure the gas flow rate. The system was gas-tight.

2.3. Sample preparation

Nine vapor samples were commercially available liquids: acetone, butanone, ethanol, methanol, isopropanol, p-xylene, benzene, ethyl acetate and diethylamine (all of which were purchased from Beijing Regent Co. Ltd.). No. 93 gasoline (premium gasoline) was obtained from a local gas station and used without further purification prior to analysis. All the FL were stored in the 500 mL bottles. The vapors were extracted by syringes from FL bottles. Then the vapors were injected into enrichment bottle firstly and then imported to the sensor array with carrier gas for detection at room temperature. The concentrations of samples were controlled at 2000 ppm. In accordance with previous studies [24,29], no significant effect is observed by adding water vapor. This indicated that the humidity has little effect on the detection results provided by the sensor array.

Real sample analysis was conducted by collecting the vapor of simulative combustion of nylon carpet (5 cm × 5 cm) infiltrated with gasoline (5 mL). The burning duration was about 120 s. The treatment process for the sample of carpet without gasoline was identical to the procedures described above.

2.4. Data collection and analysis

The CTL intensity from PMT was measured with a BPCL Ultra Chemiluminescence Analyzer (provided by Biophysics Institute of the Chinese Academy of Science). The data acquisition computer and vapor delivery system were completely integrated, enabling synchronous control of the vapor delivery and data collection. The sensor array exploits different CTL responses of nanoparticles to provide a "fingerprint" for each vapor sample; this analysis was semi-quantitative.

The CTL peak intensity patterns were analyzed by using classical linear discriminant analysis (LDA) and hierarchical cluster analysis (HCA) in SPSS (version 16.0). LDA is a robust technique for feature extraction and dimensionality reduction. It is used in finding the projection hyperplane that minimizes the interclass variance and maximizes the distance between the projected means of the classes. HCA is a method of cluster analysis which seeks to reveal natural clusters that would otherwise not be apparent within a data set.

3. Results and discussion

3.1. Choice of nanoparticles

The 10 nanoparticles, MgO, ZrO_2, CaO, γ-Al_2O_3, $Ce(NO_3)_{36}H_2O$ (ZSM-8), $Ni(NO_3)_{26}H_2O$ (ZSM-4), Al_2O_3–$Ba(NO_3)_2$–εu, Ag–BaO–Al_2O_3, Pt–BaO–Al_2O_3 and $Ba_3(PO_4)_2$, were chosen as the sensor elements of the array system because they have broad spectrum response to the sample FL vapors. Moreover, the Al_2O_3–$Ba(NO_3)_2$–εu, Ag–BaO–Al_2O_3 and Pt–BaO–Al_2O_3 catalysts present strong catalytic abilities to gasoline leading to the strongest CTL signals.

3.2. Selection of working voltage

The working temperature of sensing elements affects the performance of the CTL-based sensor array. The temperature of the heating filament was controlled by adjusting the voltage through a transformer. In array system, we could not choose a temperature exactly appropriate for each kind of nanoparticles, so the temperature selection was according to one of 10 nanoparticles′ temperature characteristics. The experimental voltage for sensor array was selected as the optimal voltage for ethanol on ZrO_2 nanoparticle as discussed in the classical experiment [25]. As shown in Fig. 2, the CTL intensities of ethanol on ZrO_2 nanoparticles were obtained by increasing the heating voltage from 4.0 V to 6.0 V. The background signal increased dramatically once the heating voltage exceeding 5.5 V, as a consequence of increasing thermal radiation. Therefore, 5.5 V (about 150 °C) was chosen as the experimental heating voltage for sensor array.

3.3. Selection of the flow rate of carrier gas

The flow rate of carrier gas affects the performance of the CTL responses by changing the concentration of vapor samples. Just like the selection of wavelength and voltage, the flow rate was

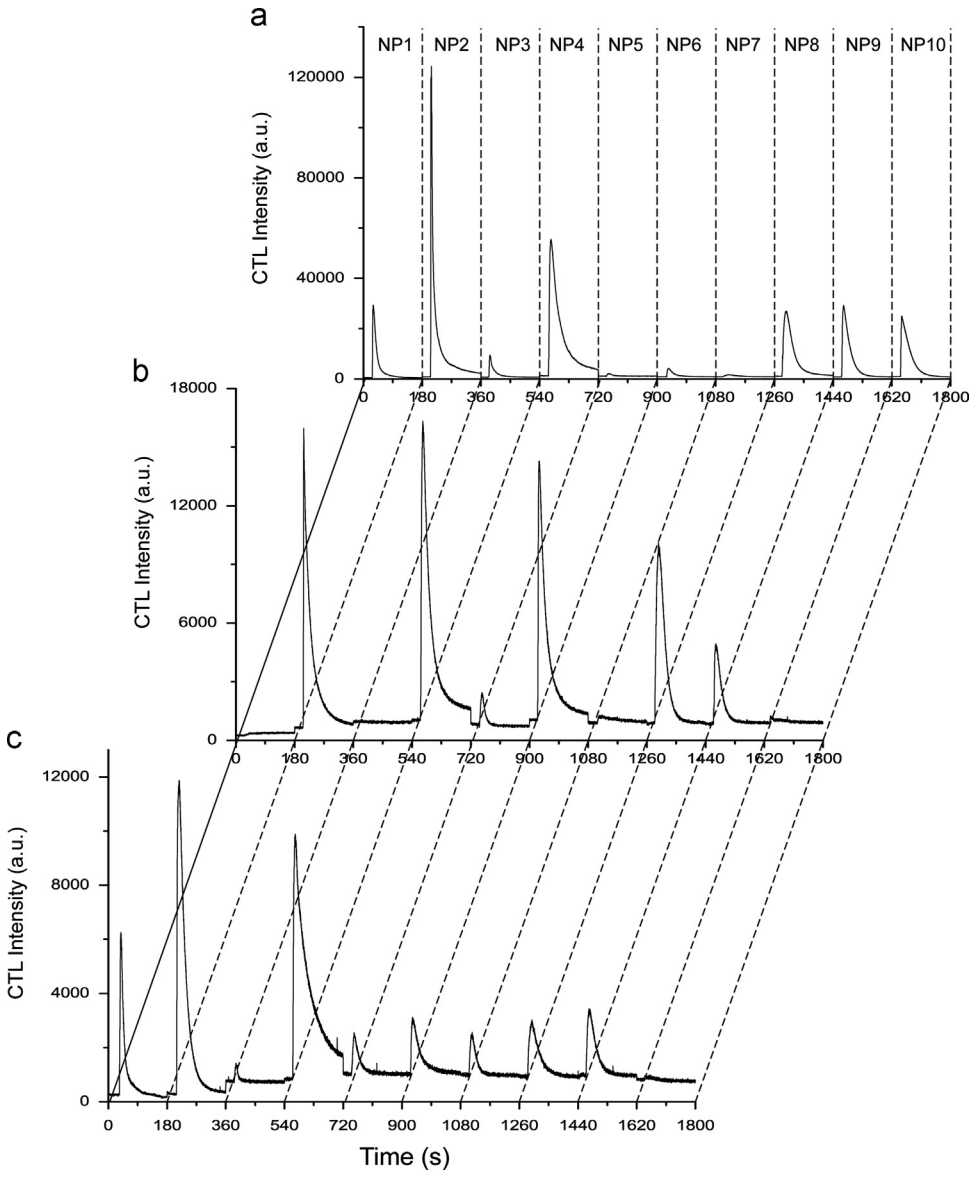

Fig. 4. The fingerprint profiles of integrate CTL responses on 10 nanoparticles for acetone (a), diethylamine (b), and gasoline (c). Nanoparticles from NP1 to NP10 are MgO, ZrO_2, CaO, γ-Al_2O_3, Pt–BaO–Al_2O_3, Ce$(NO_3)_{36}H_2O$(ZSM-8), Ni$(NO_3)_{26}H_2O$(ZSM-4), Al_2O_3–Ba$(NO_3)_2$–εu, Ag–BaO–Al_2O_3 ands $Ba_3(PO_4)_2$, respectively.

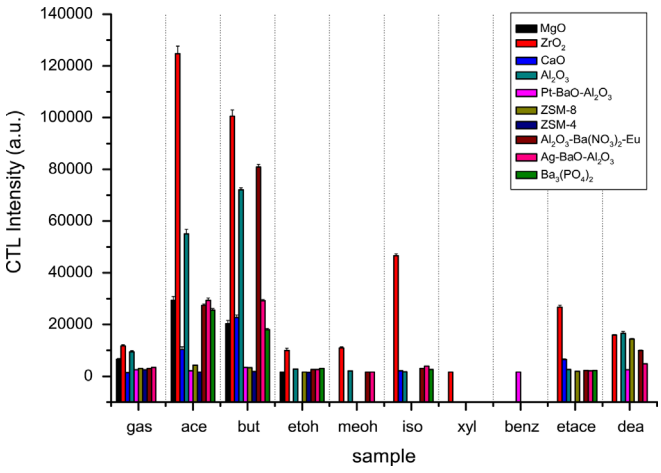

Fig. 5. CTL intensity patterns of the 10 vapor samples (2000 ppmv) on the sensor array (gas, No. 93 gasoline; ace, acetone; mek, butanone; etoh, ethanol; meoh, methanol; iso, isopropanol; xyl, xylene; benz, benzene; etace, ethyl acetate; dea, diethylamine).

determined by the choice of one kind of nanoparticles. Fig. 3 shows that the CTL intensities of ethanol vapor on ZrO_2 is enhanced gradually by increasing the flow rate from 40 to 200 mL min^{-1}, and kept relatively stable from 120 to 180 mL min^{-1}. This may be attributed to insufficient contact between the analyte and nanoparticles since the amount of vapor is not enough to reach thermodynamic equilibrium between gas and nanoparticles when the flow rate was below 120 mL min^{-1} and above 180 mL min^{-1}. For higher luminescence efficacy, a flow rate of 140 mL min^{-1} was appropriate for ZrO_2 to detect the vapor samples; the 140 mL min^{-1} was selected for the flow rate of sensor array.

3.4. CTL responses to vapors on 10 nanoparticles

To evaluate the sensing and discriminatory properties of the nanoparticles to given FL vapors, the CTL responses to vapor samples on the different types of nanoparticles were studied. For each of the three types of FL vapors on array system, we illustrate the CTL response patterns for 10 types of nanoparticles in Fig. 4. Note that acetone produces most intensive signal on ZrO_2, while weaker emission signals are produced by MgO, $Ba_3(PO_4)_2$ and no

signals are detected on ZSM-8, ZSM-4. Diethylamine generates remarkable emission on ZSM-8, but no emission is detected on MgO, ZSM-4 and $Ba_3(PO_4)_2$. Gasoline gives the abundant emission signals on MgO, ZrO_2, but only weak signals are detected on ZSM-8, ZSM-4, and there is no signal provided by $Ba_3(PO_4)_2$. The other seven vapor samples were also investigated (see Supporting information, Fig. S3). These different identification properties prompted us to develop an array system that can discriminate different vapors based on their distinct CTL intensity fingerprints. As illustrated in Fig. 5, direct injections of vapor samples (2000 ppm) to sensor array resulted in a variety of unique CTL response fingerprints, which are determined by catalytic oxidation on the surface of nanoparticles. Evidently, only gasoline, acetone, butanone and ethanol have the CTL signals on MgO, but their signals on CaO, Pt–BaO–Al_2O_3 and $Ba_3(PO_4)_2$ are different. Additionally, the CTL intensity of the butanone is the strongest on γ-Al_2O_3 of the whole vapor samples. Gasoline and ethyl acetate show analogical CTL signals on ZrO_2, CaO and γ-Al_2O_3, but very different signals on MgO, Pt–BaO–Al_2O_3, ZSM-4 and $Ba_3(PO_4)_2$. Methanol obtains no signals on MgO, CaO, ZSM-8. ZSM-4 and $Ba_3(PO_4)_2$, which is different from the other vapor samples. Xylene and benzene each has only one nanoparticle for CTL response. Diethylamine has a unique pattern of signal peaks, which has no signals on ZrO_2, CaO, ZSM-4 and $Ba_3(PO_4)_2$. Therefore, different analytes can be "fingerprinted" by their unique patterns of CTL intensities. The variation in peak intensities can be attributed to the different catalytic oxidation activities and inherent light emission performances, which depend on the characteristics of the vapor samples and nanoparticles. The outcomes are in accordance with our previous studies that the CTL emission efficiency varies for a given sample on diverse nanoparticles, and the same nanoparticle generates different CTL responses upon exposure to different analytes [22–24,26,35].

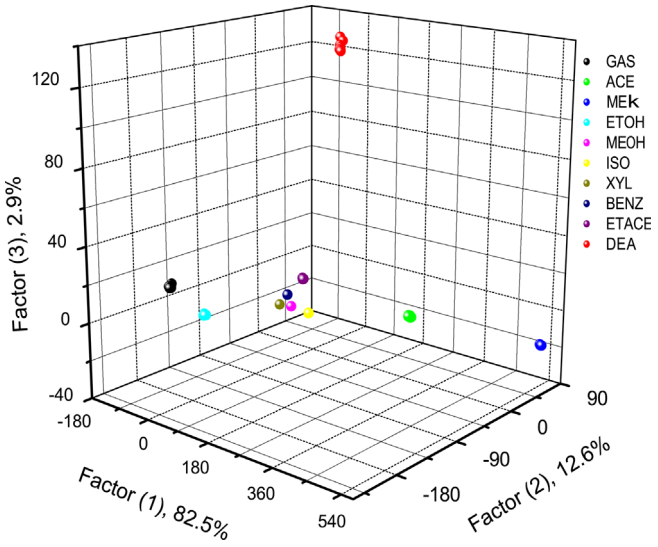

Fig. 6. Canonical score plots for the first three factors of CTL response patterns analyzed by LDA for 10 vapors.

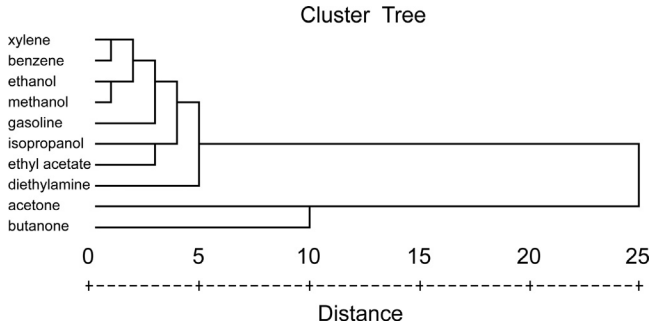

Fig. 7. Dendrogram of the CTL-based sensor array responses to 10 FL vapors. The dataset are from Fig. 5.

3.5. Pattern recognition of 10 FL vapors by CTL-based array

As shown in Fig. 6, each vapor sample obtained CTL intensities from 10 nanoparticles which were replicated seven times each, generating a data matrix for analysis. In order to examine whether these CTL patterns could be used to identify vapor samples, this multi-dimensional raw data was projected onto a three dimension space by LDA. The result is visualized as a well-clustered three-dimensional plot, and the first three canonical factors contained 82.5%, 12.6%, and 2.9% of the variation, occupying 98.0% of total variation. The result of this LDA gives us some information of the difference among vapors. The gasoline (black spheres) can be differentiated from other nine vapors as shown in Fig. 6. Acetone, butanone and diethylamine could be easily identified as well. The canonical patterns are clearly clustered into 10 different groups, and the classification accuracy is 100%.

Furthermore, we discriminated vapors by utilizing hierarchical cluster analysis (HCA) which is an exploratory tool designed to reveal natural groupings (or clusters) that would otherwise not be apparent within a dataset. The dataset from Fig. 5 was projected onto the discriminate factors obtained, and then a HCA of the new dataset of array responses was carried out. As shown in Fig. 7, a dendrogram is generated showing the difference among various FL vapors. Similar compounds, such as acetone and butanone, are

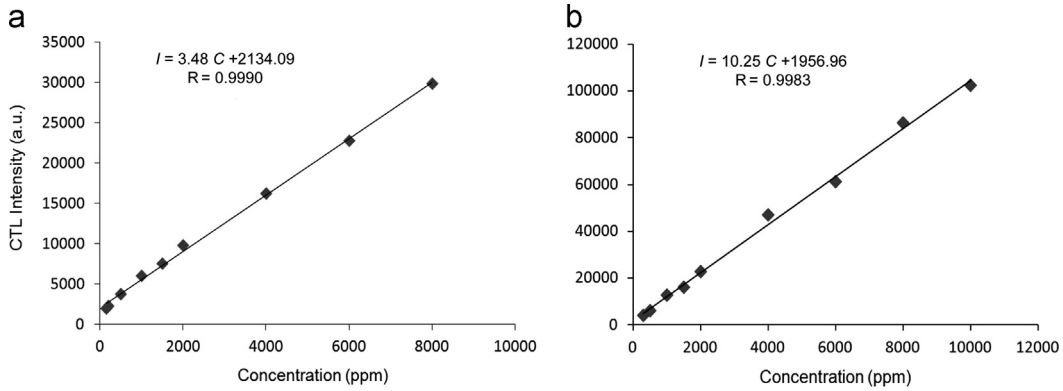

Fig. 8. The calibration curves of vapors on the sensor of CaO nanoparticle. The vapors are acetone (a) and butanone (b).

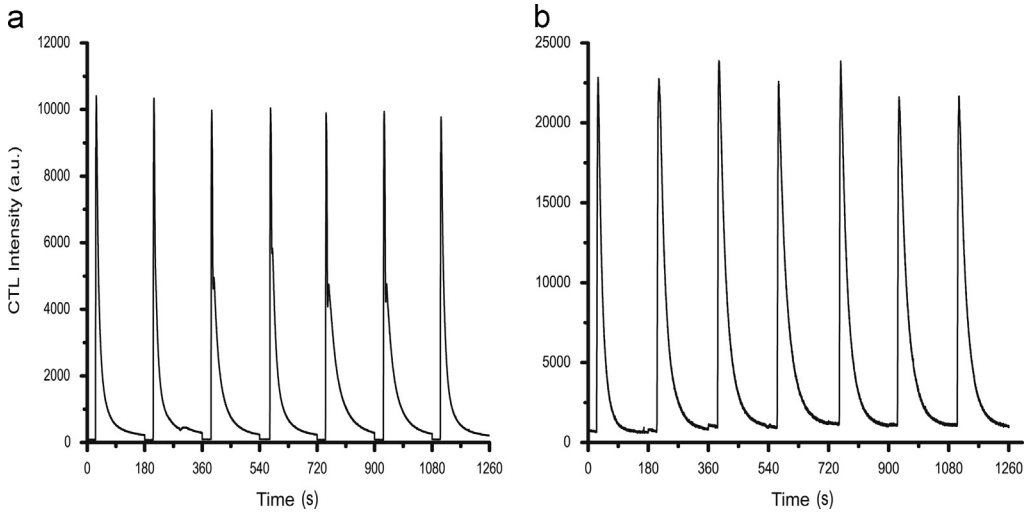

Fig. 9. Typical results obtained from seven replicate injections of vapor samples. The vapors are acetone (a) and butanone (b).

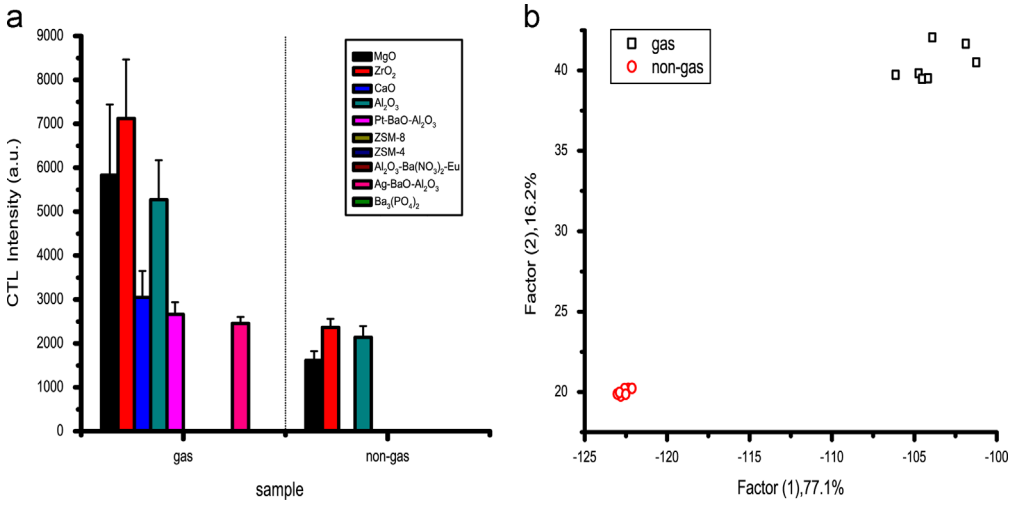

Fig. 10. The fingerprint profiles of integrate CTL responses of real combustion samples (a). Canonical score plots for the first two factors of CTL response patterns analyzed by LDA for real combustion samples (b) gas, nylon carpet with gasoline; non-gas, nylon carpet without gasoline.

classified as one category. A prominent HCA result of vapor samples was achieved with the present sensor array.

3.6. Lifetime of the sensor array

Most nanoparticles-based chemiluminescence sensors have a long-term stability since the sensing elements are solid catalysts and essentially not consumed during the sensing process. In this work, we found that the CTL-based sensor array could generate stable responses over a long time for most nanoparticles, and no significant difference in the CTL signal was observed when CTL intensities achieved at the end of the entire experiment, which lasted about two months, which agreed with our previous reports [24,26].

3.7. Analytical characteristics

Each sensing element has a different calibration curve and detection limit on each vapor sample. The quantitative analysis of vapor samples can be done only if there is one sensing element. As shown in Fig. 8, the CTL intensity varies linearly according to analyte concentration illustrated by the calibration curves of acetone and butanone on the CaO nanoparticle. The linear range of acetone and butanone are 150–8000 and 300–12000 ppm respectively. The detection limits are 60 and 90 ppm for acetone and butanone. Their linear regression equations are $I=3.48C+2134.09$ ($r=0.9980$) and $I=10.25C+1956.96$ ($r=0.9967$), where I is the CTL intensity and C is the concentration of vapors. The relative standard deviations (RSD) for 2000 ppm acetone and butanone are 2.2% and 3.7% ($n=7$), as shown in Fig. 9. However, the array containing 10 sensing elements is a semi-quantitative system, just like mammalian noses, which is not suitable for quantitative analysis. Thus, the quantitative analysis of a single analyte can be easily accomplished by comparing the achieved patterns from a library of patterns at different concentrations, but the quantitative determination of a real sample using this kind of sensor array still represents a challenge.

3.8. Real sample analysis

In order to verify the practicability of CTL-based sensor array in discrimination of real vapors, two types of stimulated fire debris samples were analyzed. One is the burned substrate (nylon carpet) with gasoline; another is the burned substrate without gasoline. As presented in Fig. 10, the difference between the CTL signals of these two types of samples is evident and the classification accuracy is 100%. This sensor array could overcome the disturbance of complex combustion background and detect residues successfully.

4. Conclusion

In conclusion, we have developed a CTL-based vapor-sensitive sensor array fabricated by 10 kinds of nanoparticles for discrimination of FL vapors. The different CTL responses of the 10 sensing elements which are collected with the array system have been used to build classification models processed by LDA and HCA. With the benefit of the reversibility and long-term stability, about two months experimental period, as well as the simple sensing elements and instrument, this array system shows great promises for use in real field detection. It is difficult to obtain a detailed characterization of the detection limit of the array system. Instead, we estimate this limit within the low parts-per-million range based on the values presented in Fig. 8. The present detection system is merely a pilot study; further research for field test is still needed. We are currently striving to extend the libraries of catalytic nanoparticles and miniaturize the instrumental apparatus.

Acknowledgments

The authors are grateful to Prof. Xinrong Zhang at The Tsinghua University for the guidance during the experiments. The authors also would like to thank Zuhe Zhang at The University of Melbourne for improving our use of English. This work is supported by 973 Program (2013CB933800) and the Ministry of Science and Technology of China (No. 2011YQ090005) Programs.

Appendix A. Supplementary material

Supplementary data associated with this article can be found in the online version at http://dx.doi.org/10.1016/j.talanta.2013.12.059.

References

[1] S. Krol, B. Zabiegala, J. Namiesnik, TRAC – Trends Anal. Chem. 29 (2010) 1092–1100.
[2] J.K. Park, H.J. Yee, S.T. Kim, Biosens. Bioelectron. 10 (1995) 587–594.
[3] Y.N. Wang, R.J. Yang, W.J. Ju, M.C. Wu, L.M. Fu, Biomicrofluidics 6 (2012) 034111.
[4] T.A. Brettell, J.M. Butler, J.R. Almirall, Anal. Chem. 83 (2011) 4539–4556.
[5] P. Mark, L. Sandercock, Forensic Sci. Int. 176 (2008) 93–110.
[6] K. Persaud, G. Dodd, Nature 299 (1982) 352–355.
[7] F. Rock, N. Barsan, U. Weimar, Chem. Rev. 108 (2008) 705–725.
[8] M. Brattoli, G. de Gennaro, V. de Pinto, A.D. Loiotile, S. Lovascio, M. Penza, Sensors 11 (2011) 5290–5322.
[9] K.J. Albert, N.S. Lewis, C.L. Schauer, G.A. Sotzing, S.E. Stitzel, T.P. Vaid, D.R. Walt, Chem. Rev. 100 (2000) 2595–2626.
[10] J.W. Grate, Chem. Rev. 100 (2000) 2627–2647.
[11] D. Matatagui, J. Marti, M.J. Fernandez, J.L. Fontecha, J. Gutierrez, I. Gracia, C. Cane, M.C. Horrillo, Sensors Actuators B – Chem. 154 (2011) 199–205.
[12] J.K. Sell, A.O. Niedermayer, S. Babik, B. Jakoby, Sensors Actuators A – Phys. 162 (2010) 215–219.
[13] F.I. Bohrer, E. Covington, C. Kurdak, E.T. Zellers, Anal. Chem. 83 (2011) 3687–3695.
[14] M.J. Aernecke, D.R. Walt, Sensors Actuators B – Chem. 142 (2009) 464–469.
[15] D.R. Walt, Curr. Opin. Chem. Biol. 14 (2010) 767–770.
[16] N. Menegazzo, B. Herbert, S. Banerji, K.S. Booksh, Talanta 85 (2011) 1369–1375.
[17] U. Beck, A. Hertwig, M. Kormunda, A. Krause, H. Krueger, V. Lohse, A. Nooke, J. Pavlik, J. Steinbach, Sensors Actuators B – Chem. 160 (2011) 609–615.
[18] Z. Weibin, P. Jung, Su, J.L. Sessler, A. Gaitas, Appl. Phys. Lett. 98 (2011) 123501.
[19] J. Long, J. Xu, Y. Yang, J. Wen, C. Jia, Mater. Sci. Eng. B – Adv. Funct. Solid-State Mater. 176 (2011) 1271–1276.
[20] M. Breysse, B. Claudel, L. Faure, M. Guenin, R.J.J. Williams, T. Wolkenstein, J. Catal. 45 (1976) 137–144.
[21] Y.F. Zhu, J.J. Shi, Z.Y. Zhang, C. Zhang, X.R. Zhang, Anal. Chem. 74 (2002) 120–124.
[22] H. Kong, S. Zhang, N. Na, D. Liu, X. Zhang, Analyst 134 (2009) 2441–2446.
[23] N. Na, S. Zhang, X. Wang, X. Zhang, Anal. Chem. 81 (2009) 2092–2097.
[24] Y. Wu, N. Na, S. Zhang, X. Wang, D. Liu, X. Zhang, Anal. Chem. 81 (2009) 961–966.
[25] F. Wen, S. Zhang, N. Na, Y. Wu, X. Zhang, Sensors Actuators B – Chem. 141 (2009) 168–173.
[26] H. Kong, D. Liu, S. Zhang, X. Zhang, Anal. Chem. 83 (2011) 1867–1870.
[27] W. Niu, H. Kong, H. Wang, Y. Zhang, S. Zhang, X. Zhang, Anal. Bioanal. Chem. 402 (2012) 389–395.
[28] Z.Y. Zhang, C. Zhang, X.R. Zhang, Analyst 127 (2002) 792–796.
[29] X.O. Cao, Z.Y. Zhang, X.R. Zhang, Sensors Actuators B – Chem. 99 (2004) 30–35.
[30] H.R. Tang, Y.M. Li, C.B. Zheng, J. Ye, X.D. Hou, Y. Lv, Talanta 72 (2007) 1593–1597.
[31] C.C. Wu, X.A. Cao, Q. Wen, Z.H. Wang, Q.Q. Gao, H.C. Zhu, Talanta 79 (2009) 1223–1227.
[32] Y.L. Wang, X.A. Cao, J.W. Li, N. Chen, Talanta 84 (2011) 977–982.
[33] M. Nakagawa, T. Okabayashi, T. Fujimoto, K. Utsunomiya, I. Yamamoto, T. Wada, Y. Yamashita, N. Yamashita, Sensors Actuators B – Chem. 51 (1998) 159–162.
[34] X. Cao, H. Dai, S. Chen, J. Zeng, K. Zhang, Y. Sun, Meas. Sci. Technol. 24 (2013) 025103.
[35] N. Na, S. Zhang, S. Wang, X. Zhang, J. Am. Chem. Soc. 128 (2006) 14420–14421.
[36] S.F. Li, J.Z. Zheng, W.X. Zhang, J. Cao, S.X. Li, Z.M. Rao, Analyst 138 (2013) 916–920.
[37] R.K. Zhang, X.A. Cao, Y.H. Liu, X.Y. Chang, Anal. Chem. 85 (2013) 3802–3806.
[38] T.A. Dickinson, J. White, J.S. Kauer, D.R. Walt, Nature 382 (1996) 697–700.
[39] M.J. Aernecke, J. Guo, S. Sonkusale, D.R. Walt, Anal. Chem. 81 (2009) 5281–5290.
[40] M.J. Aernecke, D.R. Walt, J. Forensic Sci. 55 (2010) 178–184.
[41] D. Liu, M. Liu, G. Liu, S. Zhang, Y. Wu, X. Zhang, Anal. Chem. 82 (2010) 66–68.